

Ion Yields for Tetramethylgermane Exposed to X-Rays near the Ge K-Edge

Richard A. Holroyd* and Jack M. Preses

Chemistry Department, Brookhaven National Laboratory, P.O. Box 5000, Upton, New York 11973-5000

T. K. Sham

Department of Chemistry, University of Western Ontario, London, Ontario, Canada N6A 5B7

Received: October 25, 1999; In Final Form: January 11, 2000

Free ion yields were measured for tetramethylgermane (TMG) in both the liquid and vapor phase and for Kr gas exposed to X-rays. The X-ray energy was varied across the K-edges of Ge and Kr, respectively. In Kr the relative W value increases slightly at the K-edge, which is at 14.3 keV. In liquid TMG the observed ion yield drops at the Ge K-edge (11.1 keV) and shows two minima separated by 10 eV. This ion-yield spectrum is a mirror image of the absorption spectrum, as represented by the gas-phase ion-yield spectrum. The observation of such an inverted spectrum in liquids is shown to be due in large part to inefficiency of collection of charges. This is a consequence of the large Ge cross sections above the edge which concentrates the region of irradiation near the entrance window, increasing the local dose rate and enhancing recombination. The yield of excited states in mixtures of TMG and toluene drops at the Ge K-edge by the amount expected considering the large X-ray fluorescence yield.

Introduction

Earlier conductivity studies of liquids showed that for optically thick samples, ionization yields drop suddenly at the K-edge of a constituent atom.^{1–3} Also, sharp minima in ion yield were observed at the Cl and Si K-edges in liquid CCl₄ and Si(CH₃)₄.^{1,2} Inverted EXAFS spectra were obtained at the iron K-edge for a solution of ferrocene in 2,2,4-trimethylpentane.³ Various reasons have been proposed to explain these apparent low yields at and above edges.

In this study samples of tetramethylgermane and krypton are exposed to X-rays. The X-ray energy is scanned across the respective K-edge, and yields of ionization and excitation resulting from electron emission are measured. Experiments are done with gases to determine if the W value for photons, the number of eV necessary to produce an ion pair, changes across a K-edge. This also provides an estimate of the initial yields of ions in the liquid. The total energy released in electrons is nearly the same just below and above a K-edge, but the fraction of energy going into photoelectrons and Auger electrons of different energies changes. Some changes in W , amounting to as much as 5%, were observed across the carbon K-edge in methane.⁴ Theoretical Monte Carlo simulations have indicated that small changes in W are to be expected at the L-edge of gaseous xenon.⁵ Experimental W values have been measured for noble gases at individual X-ray lines.^{6,7} In the case of Xe, one study used line sources on either side of the L_{III}-edge and W was found to be the same within experimental error.⁷ Studies at the Xe K-edge showed a discontinuity at the edge, which indicate that W is about 0.5% higher above the edge than below.⁶ Any fine structure in W at the K-edge would not have been detected in these studies.

Energetic photoelectrons produce many ionizations and excitations. For example, a single 10 keV electron will generate about 400 ion pairs initially. Below an edge, the resulting photoelectron receives most of the energy of the photon. At

and above an edge the absorbed energy resides either in the electrons of the Auger cascade or is emitted as fluorescence. Photoelectrons and Auger electrons of comparable energies, should be equally effective in ionizing the liquid. This study was designed to determine the reason for the observed edge effects: whether the observed drops in ion yield are due to some fundamental change in the primary process lowering the ion yield in the Auger process or whether the effect is caused by inefficient collection of ions.

Experimental Section

The experiments described here were done at beamline X7B at the National Synchrotron Light Source (NSLS). A Si 311 crystal monochromator that produced the narrowest available radiation was used in order to best reveal edge structure. The reported resolution is 0.56 eV at 10 keV. This monochromator has the added advantage of rejecting second-order radiation, which was significant because the X-ray ring at the NSLS was running at 2.8 GeV. Beam intensity was monitored with an N₂-filled ion chamber preceding the sample cell. The beam entered the ion chamber through a variable slit so as to maximize ion collection efficiency (see below). The X-ray intensity emerging from the ion chamber, I_0 , calculated from the ion chamber current i_0 , is given by

$$I_0 = \frac{i_0 W(N_2)R}{qE_X} \text{ photon/s} \quad (1)$$

Here, $W(N_2) = 35.8$ eV/ion pair,⁸ q is the electronic charge, E_X is the X-ray energy, and R is the ratio of photons transmitted to photons absorbed, given by $\exp(-\rho_N \sigma_N d) / [1 - \exp(-\rho_N \sigma_N d)]$, where ρ_N is the nitrogen density, σ_N the (energy dependent) nitrogen cross section,⁹ and d is the length of the ion chamber. Ion yields in TMG were determined using a 3-cm long cell, which is described elsewhere.¹⁰ The cell was placed immediately

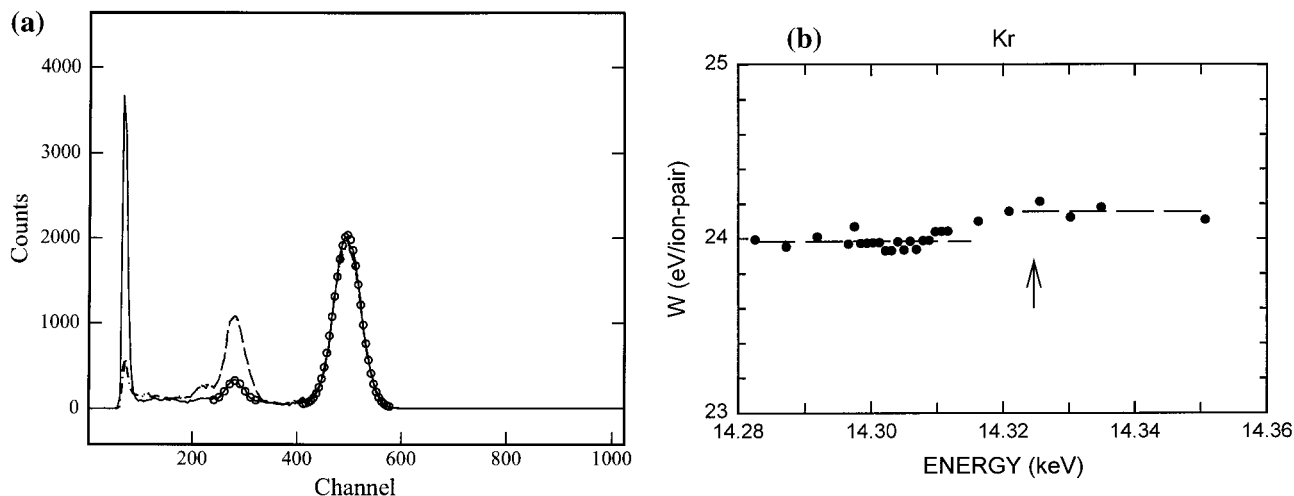


Figure 1. (a) Multichannel analyzer spectra. Solid line obtained at 14.339 keV; dashed line at 14.283 keV. The main Auger peak is centered at channel 496. (b) Relative W value of Kr gas versus X-ray energy. Kr K-edge indicated by arrow.

behind the ion chamber. The electrodes in the cell are parallel to the beam and separated by 3 mm.

The liquids used in this experiment, tetramethylgermane (Gelest), 2,2,4,4-tetramethylpentane (Wiley 99.99%), and toluene (Wiley 99%), were dried prior to use by passage through activated silica gel.

Ultraviolet fluorescence was measured across the Ge K-edge for solutions of TMG containing toluene. A 295-nm interference filter (Corion) was used to cut out stray light and pass the fluorescence, which was detected by a photomultiplier tube (Amperex 1003). The fluorescence yield is a relative measure of the yield of excited states since beam intensity was monitored as above.

A proportional counter, described elsewhere,¹¹ was used to measure the number of ions per photon across the K-edge of Kr. This technique requires low counting rates, which were attained by adjusting the input slit to pass only a fraction of the flux. The signal from the counter was amplified using an Ortec 460 delay line amplifier. Pulses were accumulated in a calibrated multichannel analyzer (LeCroy 3500).

Results and Discussion

Gas-Phase Ion Yields – Kr. Spectra obtained with a gas mixture of 90% Kr and 10% CO₂ in the counter are shown in Figure 1a. The solid line spectrum was obtained at an X-ray energy of 14.339 keV, above the K-edge which is at 14.326 keV. The main peak is centered at channel 496. The small peak at channel 282 results from fluorescence emission due to the primary X-rays impinging on the Cu electrode in the rear of the detector. The dashed line spectrum was obtained at 14.283 keV, below the edge. The main peak is in the same position, but the Cu fluorescence peak is stronger because the primary X-ray beam is more penetrating. Similar spectra were accumulated at small energy increments across the K-edge. Since the peak position is proportional to the number of ion pairs created, the X-ray energy divided by the channel number is a relative measure of the W value. These results are shown in Figure 1b where the data have been normalized at the lowest energy to the known W value for Kr of 24.0 eV/ion pair reported for 5.9 keV X-rays.⁷ The W value is slightly higher (by 0.7%) at X-ray energies above the edge. Thus, our results are not inconsistent with the results obtained for Xe which showed a 0.5% change at the K-edge. Because there is some scatter in these measurements, a more careful study would be needed to

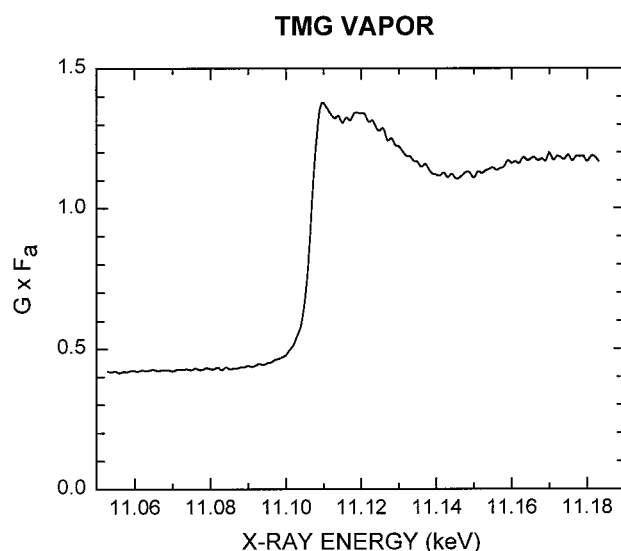


Figure 2. Product of ion yield times fraction absorbed vs X-ray energy for TMG vapor.

confirm this small jump. The inverse of the W value gives the ion yield ($G = 100/W$) in ions/100 eV.

TMG Vapor. The ionization current for TMG vapor was measured in the 3-cm cell. Because the absorption is weak, the ionization spectrum has the appearance of an absorption spectrum and the observed current increases at the K-edge (Figure 2). This spectrum resembles the published transmission spectrum of a thin cell of liquid TMG showing two peaks separated by 10 eV; the main peak is attributed to a $\sigma^*(\text{Ge}-\text{C})$ resonance.¹²

To derive the yield of ion-pairs (G) the cell current i_c is divided by q , the X-ray intensity I_0 , the X-ray energy, the fraction of the beam transmitted by the cell window F_w , and the fraction of X-rays absorbed by the sample F_a , or

$$G = \frac{100i_c}{E_X q I_0 F_w F_a} \text{ ion pairs/100 eV} \quad (2)$$

When I_0 , defined by eq 1, is combined with eq 2, G is shown to be a function of the ratio i_c/i_0 :

$$G = \frac{100i_c}{i_0 W R F_w F_a} \text{ ion pairs/100 eV} \quad (3)$$

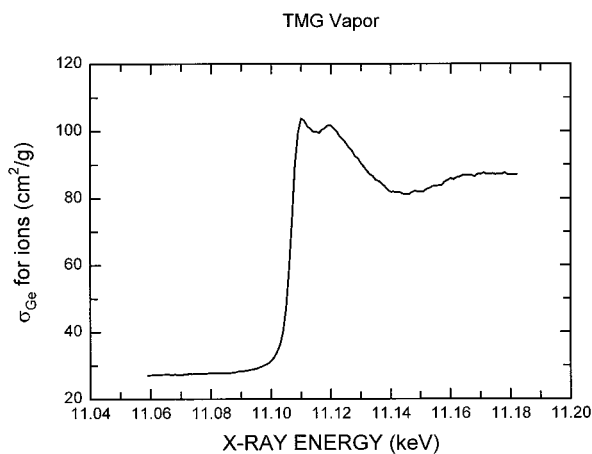


Figure 3. Ge cross section vs energy derived from the ion yield spectra.

The curve shown in Figure 2 is actually a plot of $G \times F_a$; i.e., the data are not divided by F_a . This fraction absorbed can be calculated from cross section and density data.

$$F_a = 1 - \exp[-3 \times (\rho_C \sigma_C + \rho_H \sigma_H + \rho_{Ge} \sigma_{Ge})] \quad (4)$$

The ρ s are the densities of each atom in g/cm^3 and the σ s are the energy dependent cross sections in cm^2/g .⁹

First, the spectrum of $G \times F_a$ was used to calculate the value of G for the vapor. Published cross sections⁹ along with densities, based on the vapor pressure of TMG at 22 °C of 0.416 atm, were substituted into eq 4 to calculate F_a . The result for energies below the edge is $G = 4.2$ ion pair/100 eV. This value is quite reasonable since the W value for various gaseous hydrocarbons is between 23 and 25 eV,¹³ corresponding to $G = 4$ to 4.3 ion pairs/100 eV.

These data were used in another way by assuming the value of $G = 4.2$ ion pair/100 eV applies throughout the spectrum and calculating F_a , and subsequently σ_{Ge} from F_a , by inverting eq 4. The assumption of a constant G is reasonable, based on the invariance of the W value of Kr across the Kr-edge as reported above. A more realistic Ge cross section, as shown in Figure 3, is thereby obtained which shows the fine-structure near the K-edge. Below the edge, the cross section is the same as tabulated values. Above the edge the cross section is roughly one-half that reported because it represents the Auger part of the cross section, the fluorescent X-rays mostly escape when the cell contains only vapor.

Liquid TMP Ion Yields. Measurements were made with liquid 2,2,4,4-tetramethylpentane (TMP) in order to show that the ions were efficiently collected in this case. TMP and TMG are similar electronically in that the free ion yields are comparable and the electron mobilities are high in both.¹⁴ For a parallel plate ionization detector, the collection efficiency F is given by eq 5; although derived for the gas phase, this equation applies equally well to liquids. F depends strongly on the electric field E , the slit width L , and the dose rate Q :¹⁵

$$F = \frac{2}{1 + \sqrt{1 + \frac{4qL^2Q}{3\epsilon_0\epsilon_r E^2\mu}}} \quad (5)$$

The ion mobility μ and dielectric constant ϵ_r are fixed values for each liquid. To maximize F the dose rate needs to be minimized and L should be small. In the case of TMP the X-rays are not totally absorbed by the 3-cm cell. The $1/e$ depth of penetration of the X-rays is ≈ 1 cm. This spreads out the

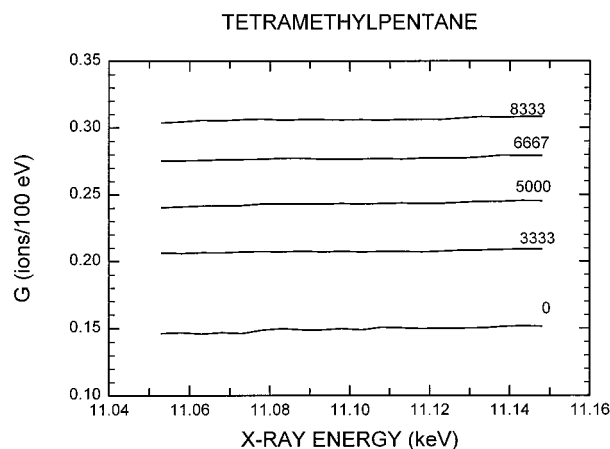


Figure 4. Free ion yield vs X-ray energy for liquid 2,2,4,4-tetramethylpentane. Electric field (in V/cm) indicated on figure.

ionization density and minimizes Q . Efficiencies of collection were estimated to be 98% or better for TMP.

Figure 4 shows spectra of $G(\text{ion})$ for TMP taken in 5 eV steps in the vicinity of the Ge K-edge. The results for four voltages are shown. The change in $G(\text{ion})$ over the X-ray energy range studied is small. G is assumed to be linearly dependent on electric field (E), as in eq 6

$$G = G^0 + S \times E \quad (6)$$

The average value of the slope-to-intercept ratio, S/G^0 , equals 1.26×10^{-4} cm/volt, in reasonable agreement with previous results² and that expected from Onsager theory. Such a linear dependence is also predicted to apply to multiple ion-pair spurs.¹⁶ The y-intercept yields G^0 , obtained by extrapolation of the data at the three highest voltages. The yield increases very slightly with increasing energy, as expected (see lower line in Figure 4); the average value is $G^0 = 0.15$ ions/100 eV. A computer simulation, based on an exponential distribution of separation distances of 26.5 nm, predicts $G = 0.158$ ions/100 eV for 11.1 keV.¹⁷ This computer simulation is in good agreement with other experimental ion yield data for TMP for X-ray energies from 2 to 2000 keV.

Liquid TMG – Ion Yields. Similar experiments were done with liquid TMG as a function of X-ray energy to measure the yield of free ions across the K-edge of Ge at 11.1 keV. The results obtained at applied voltages of 1000 and 2000 V are shown in Figure 5. It is apparent that these spectra are nearly a *mirror image* (about a horizontal plane) of the gas phase spectra (Figure 2a). The yield drops, instead of rising, at the K-edge, and the two peaks separated by 10 eV in the gas phase appear as minima in the liquid. In addition to this structure, the yield of ions is lower above the edge than it is below. In all the liquid TMG experiments the X-ray beam is totally absorbed.

The data were fit to eq 6 as was done for TMP to obtain G^0 . Data at only the highest three voltages were used. The yield below the edge was $G^0 = 0.092$ per 100 eV and the S/G^0 ratio = 1.03×10^{-4} cm/volt. The X-rays are strongly absorbed here because of the larger cross section of Ge. Actually, below the edge Ge accounts for 96% of the absorption and the half-depth of penetration is only 0.045 cm. The experimental conditions were similar to those used for TMP, consequently the dose rate Q was significantly higher. The use of eq 5 showed, however, that the collection efficiency was better than 97% for applied fields of 5 kV/cm or more. The value of $G^0 = 0.092/100$ eV is reasonable compared to that for TMP. In general, ion yields are less for Ge or Si substituted compounds than for similar

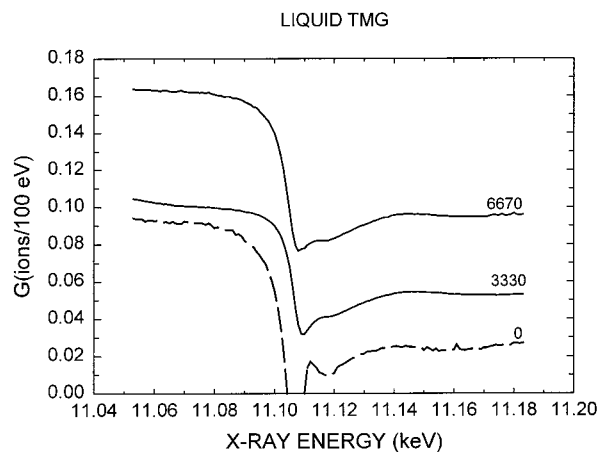


Figure 5. Free ion yield vs X-ray energy for liquid tetramethylgermane at applied fields (V/cm) indicated.

hydrocarbons.¹⁴ At and above the K-edge the extrapolated G^0 values are much lower. The extrapolated yields at the first minimum are near zero and the yields above the edge are well below that expected.

Collection Efficiency. To explain the low ion yields above the K-edge and the mirror-like appearance of the liquid ion spectra, as compared to the vapor, we first consider collection efficiency as a cause. The observed currents can be regarded as a real current times the experimental collection efficiency. In a given spectral scan, the X-ray flux is roughly constant and of course the applied voltage and slit width are constant. At the edge, the irradiated volume decreases. Above the K-edge the Ge cross section is much larger and the beam penetrates a shorter distance into the liquid. The dose rate Q also drops off exponentially from the front window and the collection efficiency will be lowest near the window and higher farther into the cell where the dose rate is less. To estimate the distance dependence of F we can rewrite eq 5 as

$$F(x) = \frac{2}{\left[1 + \left(1 + C \frac{dQ}{dx}\right)^{1/2}\right]} \quad (7)$$

where $C = (4qL^2)/3\epsilon_0\epsilon_r E^2\mu$, and dQ/dx is the differential dose rate in some rectangular slice parallel to the front window. In general, $C(dQ/dx)$ is small, therefore $F(x)$ can be estimated to first order as

$$F(x) = 1 - \frac{C}{4} \frac{dQ}{dx} \quad (8)$$

at any point x from the window. The dose rate is calculated from the X-ray intensity I_0 , given by eq 1. The intensity on the front surface of the liquid is $I_0 \times F_w$. To calculate the absorbed dose, I_0 is multiplied by the X-ray energy and $G(\text{ions})$, and divided by 100 times the beam area (A)

$$Q = B[1 - \exp(-\sigma_{\text{Ge}}\rho_{\text{Ge}}x)] \quad (9)$$

where $B = i_0 W R F_w (G/100qA)$, then

$$\frac{dQ}{dx} = B\sigma_{\text{Ge}}\rho_{\text{Ge}} \exp(-\sigma_{\text{Ge}}\rho_{\text{Ge}}x) \quad (10)$$

The parameter B includes terms such as R and F_w that vary slowly with photon energy. It also includes G , which may vary. Based on the constancy of W across the K-edge of Kr (Figure 1b), we take G to be constant.

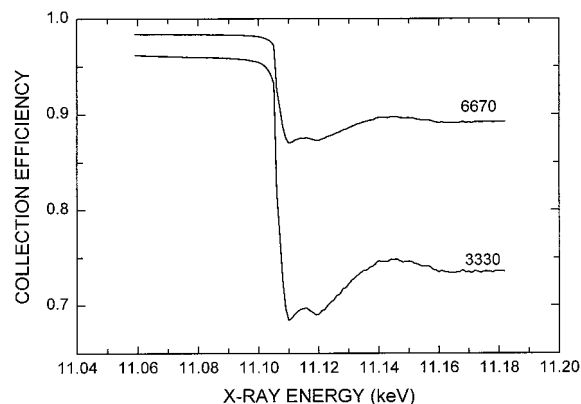


Figure 6. Calculated average collection efficiencies vs X-ray energy for TMG at two applied fields.

Since the collection efficiency varies with distance, we calculated the average efficiency given by

$$\bar{F} = \frac{\int_0^3 F(x) \frac{dQ}{dx} dx}{\int_0^3 \frac{dQ}{dx} dx} \quad (11)$$

When integrated, eq 11 simplifies to

$$\bar{F} = 1 - \left(\frac{BC}{8}\right)\sigma_{\text{Ge}}\rho_{\text{Ge}} \quad (12)$$

using the definitions in eqs 8 and 10. Thus, to first order the efficiency follows σ_{Ge} and is expected to decrease when σ_{Ge} increases and vice versa. The cross sections and densities of carbon and hydrogen are included in the calculation but have been omitted in the equations for clarity. Actually, germanium dominates, absorbing 96% below the edge and >99% above. Figure 6 shows average efficiency curves for the conditions of the measurements in Figure 5. There is a marked similarity of the two figures; the drop in efficiency is larger at lower applied voltage. If the yield of ions, G , is corrected for the inefficiency of collection, we find the yield of ions above the edge is $65 \pm 5\%$ of the yield below the edge. A value around 73% is to be expected since the absorption is so close to the front window that about 50% of the fluorescent X-rays would escape and the fluorescence quantum yield is 0.535.¹⁸ This shows that inefficiency of ion collection is the major cause of the inverted ion yield curves observed for TMG.

Dilution Experiments. Since the X-rays are absorbed close to the window, dilution experiments were also done to see if edge structure is preserved with dilution, which would spread out the irradiated zone and decrease the dose rate. 2,2,4,4-tetramethylpentane was used for dilution. For 10% TMG, the half-depth of penetration of the X-rays is 0.27 cm below the edge and 0.05 cm above. The results for a 10% TMG sample are shown in Figure 7b; the field applied in this case was 5000 V/cm. Below the edge, the efficiency of collection is high and $G(\text{ions})$ is 0.17 per 100 eV. This value is intermediate between the value observed for neat TMG at this voltage (0.14) and the value observed for TMP (0.24).

Above the K-edge there is still an approximately 50% drop in the yield, and some of the same structure is still observed at the edge. The calculated efficiency of collection in this case is better than 95% as shown in Figure 7a. The reason for the lower yield above the edge can be attributed to the loss of the fluorescent X-rays. A little over 50% of the absorbed photons lead to X-ray fluorescence. The energies of the fluorescent

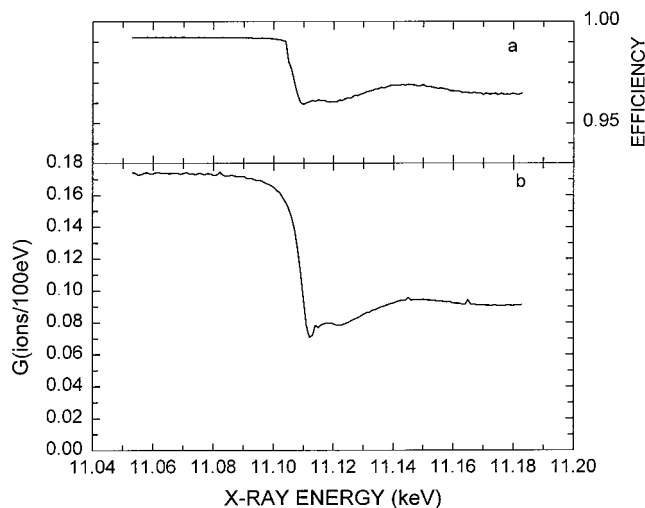


Figure 7. Data for 10% TMG in TMP. (a) Calculated ion collection efficiency vs energy. (b) Measured ion yield across the Ge K-edge.

X-rays, at 9.9 and 11 keV,⁹ are below the edge where the cross section for absorption is smaller. Since the X-rays are absorbed close to the window above the edge, most of the fluorescence emitted backward will be lost. Roughly half of the fluorescence emitted forward will be lost because the electrodes were only 0.15 cm from the beam and the half-depth for fluorescent photons is 0.27 cm. Thus, the yield observed above the edge is approximately what is expected.

At the K-edge the minima at 11.11 and 11.12 keV can still be seen. The calculated efficiency curves also show these dips. Quantitatively, the yields drop to 0.07 ions/100 eV, more than expected. Nevertheless, since the drop in yield is small we have no reason to suggest an alternative explanation. On the other hand, we cannot totally rule out a small contribution from a change in primary process at the σ^* resonance. For example, there may be a change in yield of fluorescence from these excited states causing fewer ions to be observed.

UV Fluorescence Experiments. Fluorescence was also measured across the Ge K-edge for samples of TMG containing toluene. Excited states are formed largely as a result of ion recombination of cations with electrons or anions



This happens mostly in the track of the photoelectron, and both singlet and triplet excited states will be formed. The excited singlet state of toluene can be detected by its fluorescence at 295 nm. The experiment is done in the absence of an electric field so that all ions recombine. The fluorescence yield should then be a measure of the total yield of excited states. The results for 20% TMG in toluene are shown in Figure 8. At the edge, the yield drops by about 25%. The decrease is approximately what is expected, because above the edge the Auger yield is only 0.46. The rest of the yield consists of fluorescent X-rays, about half of which escape because the absorption occurs close to the entrance window; the half-depth of incident X-rays is 0.03 cm. for this solution.

EXAFS Spectra. EXAFS spectra can be obtained by conductivity as indicated in the Introduction. Figure 9 shows such a plot of the ratio of the cell current (i_c) to the ion chamber current (i_0) for liquid TMG with a voltage of 2.5 keV applied. Structure is observed to 400 eV above the edge, but peaks in the absorption spectrum appear here as dips in the ratio i_c/i_0 . This inverted spectrum is explained in the same way as the ion-yield spectrum. When the Ge cross section increases, the

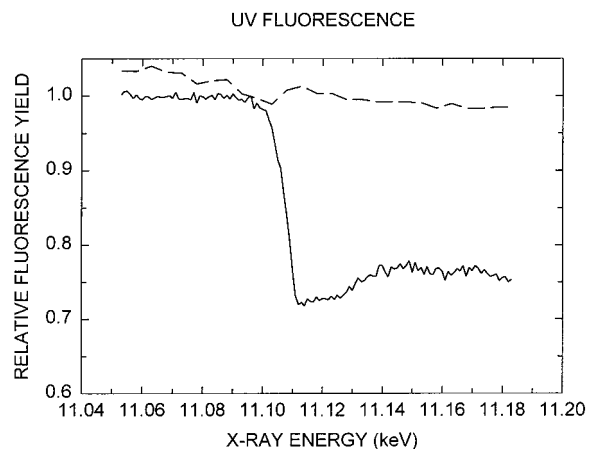


Figure 8. Relative UV fluorescence yield vs energy. Dashed line is for pure toluene; solid line is for 20% TMG in toluene.

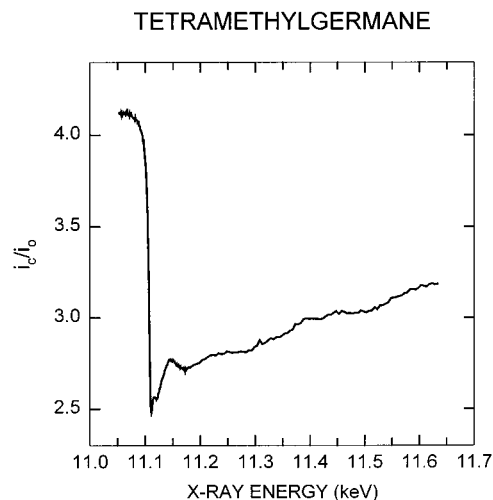


Figure 9. EXAFS-type spectrum (i_c/i_0) for liquid tetramethylgermane; applied field 1667 V/cm.

collection efficiency decreases proportionately and the current is lower. Even though inverted, such spectra provide valid structural information.³

Summary

This study shows that the inefficiency of collection, which scales as the Ge cross section, accounts for the low yield of ions above the K-edge of Ge in liquid TMG as well as the minima observed near the edge. This effect probably also explains the similar inverted spectra observed in tetramethylsilane² and carbon tetrachloride¹ because of the large cross sections of Si and Cl, above their respective K-edges. Changes in initial yield of ions across the K-edge can be ruled out as a significant cause of structure in the spectra.

Acknowledgment. The authors thank Jonathan C. Hanson for his assistance in utilizing the X7B beamline at the NSLS and Graham Smith for assisting with the Kr W value measurements. This research was carried out at Brookhaven National Laboratory and supported under contract DE-AC02-98-CH10886 with the U.S. Department of Energy and supported by its Division of Chemical Sciences, Office of Basic Energy Sciences.

References and Notes

- (1) Holroyd, R. A.; Sham, T. K.; Yang, B.-X.; Feng, X.-H. *J. Phys. Chem.* **1992**, *96*, 7438.
- (2) Holroyd, R. A.; Sham, T. K. *Radiat. Phys. Chem.* **1998**, *51*, 37.

- (3) Sham, T. K.; Holroyd, R. A. *J. Chem. Phys.* **1984**, *80*, 1026.
- (4) Suzuki, I. H.; Saito, N. *Bull. Chem. Soc. Jpn.* **1985**, *58*, 3210. Saito, N.; Suzuki, I. H. *Chem. Phys.* **1986**, *108*, 327.
- (5) Dias, T. H. V. T.; Santos, F. P.; Stauffer, A. D.; Conde, C. A. N. *Phys. Rev. A* **1993**, *48*, 2887.
- (6) (a) dos Santos, J. M. F.; Morgado, R. E.; Tavora, L. M. N.; Conde, C. A. N.; *Nucl. Instr. Methods A* **1994**, *A350*, 216. (b) Tsunemi, H.; Hayashida, K.; Torii, K.; Tamura, K.; Miyata, E.; Murakami, H.; Ueno, S. *Nucl. Instr. Methods A* **1993**, *336*, 301.
- (7) Borges, F. I. G. M.; Conde, C. A. N. *Nucl. Instr. Methods A* **1996**, *A381*, 91.
- (8) Srdoč, D.; Inokuti, M.; Krajcar-Bronić, I. In *Atomic and Molecular Data for Radiotherapy and Radiation Research*; IAEA-TECDOC-799, 1995; (a) p 569, (b) p 610.
- (9) McMaster, W. H.; Kerr, N.; Del Grande, N. K.; Mallet, J. H. Hubbell, J. H. *Compilation of X-ray Cross Sections*, UCRL-50174. Storm, E.; Israel, H. I. *Nucl. Data Sect. A* **1970**, *7*, 565.
- (10) Holroyd, R. A.; Sham, T. K. *J. Phys. Chem.* **1985**, *89*, 2909.
- (11) Smith, G. C. *NIM Phys. Res.* **1984**, 222, 230.
- (12) Hitchcock, A. P.; Tyliczak, T.; Aebi, P.; Xiong, J. Z.; Sham, T. K.; Baines, K. M.; Mueller K. A., Feng, X.-H.; Chem, J. M.; Yang, B. X.; Lu, Z. H.; Baribeau J.-M.; Jackman, T. E. *Surf. Sci.* **1993**, *291*, 349.
- (13) Meisels, G. G. *J. Chem. Phys.* **1964**, *41* 55.
- (14) Gear, S.; Holroyd, R. A.; Ptohos, F. *Nucl. Instr. Methods* **1991**, *A301*, 61.
- (15) Hine, G. J.; Brownell, G. L. *Radiation Dosimetry*; Academic Press: NY, **1956**, p 165.
- (16) Pimblott, S. *J. Chem. Soc., Faraday Trans.* **1993**, *89*, 3533.
- (17) Siebbeles, L. D. A.; Bartczak, W. M.; Terrissol, M.; Hummel, A. *J. Phys. Chem.* **1997**, *101*, 1619.
- (18) Krause, M. O. *J. Phys. Chem. Ref. Data* **1979**, *8*, 307.